INFECTION AND IMMUNITY, Jan. 1996, p. 319–325
0019-9567/96/$04.00+0

Vol. 64, No. 1

Intracellular Fate of *Mycobacterium avium*: Use of Dual-Label Spectrofluorometry To Investigate the Influence of Bacterial Viability and Opsonization on Phagosomal pH and Phagosome-Lysosome Interaction

YU-KYOUNG OH† AND ROBERT M. STRAUBINGER*

Department of Pharmaceutics, State University of New York at Buffalo, Amherst, New York 14260

Received 13 January 1995/Returned for modification 27 February 1995/Accepted 1 September 1995

Mycobacterium avium **is a facultative intracellular pathogen that can survive and replicate within macrophages. We tested the hypotheses that survival mechanisms may include alteration of phagosomal pH or inhibition of phagosome-lysosome fusion. *M. avium* was surface labeled with *N*-hydroxysuccinimidyl esters of carboxyfluorescein (CF) and rhodamine (Rho) to enable measurement of the pH of individual *M. avium*-containing phagosomes and the interaction of bacterium-containing phagosomes with labeled secondary lysosomes. CF fluorescence is pH sensitive, whereas Rho is pH insensitive; pH can be calculated from their fluorescence ratios. Surface labeling of *M. avium* did not affect viability in broth cultures or within J774, a murine macrophage-like cell line. By fluorescence spectroscopy, live *M. avium* was exposed to an environmental pH of ≈5.7 at 6 h after phagocytosis, whereas similarly labeled *Salmonella typhimurium*, zymosan A, or heat-killed *M. avium* encountered an environmental pH of <5.0. Video fluorescence and laser scanning confocal microscopy gave consistent pH results and demonstrated the heterogeneity of intracellular fate early in infection. pH became more homogeneous 6 h after infection. *M. avium* cells were coated with immunoglobulin G (IgG) or opsonized to investigate whether phagocytosis by the corresponding receptors would alter intracellular fate. Opsonized, unopsonized, and IgG-coated *M. avium* cells entered compartments of similar pH. Finally, the spatial distribution of intracellular bacteria and secondary lysosomes was compared. Only 18% of live fluorescent *M. avium* cells colocalized with fluorescent lysosomes, while 98% of heat-killed bacteria colocalized. Thus, both inhibition of phagosome-lysosome fusion and alteration of phagosomal pH may contribute to the intracellular survival of *M. avium*.**

Mycobacterium avium can survive in macrophages and causes one of the most common opportunistic infections in AIDS patients (7, 18). In spite of its clinical prevalence, it is unclear how *M. avium* survives in the phagocytic cells that can otherwise kill a variety of microorganisms by using various antimicrobial host defense systems.

One major killing mechanism of macrophages is the acidification of pathogen-containing phagosomes to pH <5, under which conditions the activity of lysosomal enzymes is optimal and the survival of many microorganisms is diminished. To cope with these potentially lethal conditions, pathogens employ various survival strategies. Escape from acidified phagosomes into the cytoplasm has been reported for the intracellular pathogens *Listeria monocytogenes* and *Shigella* spp. (8). Reduced phagosomal acidity was also implicated in the survival of *Legionella pneumophila* (9) and *Toxoplasma gondii* (16).

Recently it was reported that *M. avium* labeled with a pH-sensitive fluorescent probe resides in macrophages in an environment that is less acidic than in lysosomes (17). However, fluorometry is a population average method which obscures information on the possible heterogeneity of the environmental pH among phagosomes, and asynchrony in the intracellular processing of bacteria may blunt the observed rate of vacuole acidification.

In the present study, we tested the hypothesis that survival of *M. avium* involves the localization of bacteria in a less acidic vacuolar compartment and the hypothesis that derangements in phagosome-lysosome interaction may contribute to intracellular survival. Bacteria were surface labeled with carboxyfluorescein (CF) and carboxytetramethyl rhodamine (Rho), dual fluorescent probes that allowed accurate measurement of the pH surrounding the bacteria in macrophages. CF emission intensity, like that of fluorescein, varies with pH, with an apparent pK_a of ≈6.1. Therefore, the spectral changes of CF are maximal in the pH range relevant to changes occurring in the endocytic pathway. Rho fluorescence is relatively insensitive to pH; Rho thus provides a reference signal that allows calculation of pH from the ratio (14) of CF and Rho fluorescence.

Ratio methods employing fluorescein or closely related derivatives such as CF have been used previously to measure pH in the endocytic pathway (13–15) by comparing the fluorescence detected from both pH-sensitive and -insensitive domains of the excitation or emission spectrum in order to calculate pH. The advantage of ratio methods is that the pH-invariant reference signal obviates the requirement that the probe concentration be known or constant in each cellular compartment. Although the fluorescein spectrum has both pH-sensitive and -insensitive regions in its excitation spectrum (15), fluorescence emission at the pH-insensitive wavelengths is weak, and fluorescein lacks a consistent isosbestic wavelength. In addition, the pH-sensitive and reference wavelengths are relatively closely spaced, posing difficulties for use

* Corresponding author. Mailing address: Department of Pharmaceutics, 539 Cooke Hall, SUNY at Buffalo, Amherst, NY 14260. Phone: (716) 645-2844, ext. 243. Fax: (716) 645-3693. Internet: rms@acsu.buffalo.edu.

† Present address: Department of Cell Biology, Harvard Medical School, Boston, MA 02115.

in fluorescence microscopy; filters or laser sources may not provide the optimal wavelengths for the determination of pH. The employment of a second, spectrally distinct reference fluorophore such as Rho provides separation of the pH-sensitive and reference signals into regions of the spectrum that are easily achieved with conventional lasers. Furthermore, the ability to vary the ratio of the probes allows matching the assay to the dynamic range of the video or photomultiplier detectors, thereby providing greater accuracy in the pH measurement.

Fluorometry, video fluorescence microscopy, and confocal laser scanning microscopy were used to investigate the rate and degree of acidification of intracellular vacuoles containing either live or heat-killed *M. avium*. We also investigated the optimal pH for the growth of *M. avium* in order to estimate the effect of phagosomal pH on bacterial viability. Finally, we studied the role of several macrophage surface receptors in the subsequent intracellular processing of *M. avium.*

MATERIALS AND METHODS

Materials. *N*-Hydroxysuccinimidyl (NHS) 5- (and -6)-carboxyfluorescein (NHS-CF) and *N*-hydroxysuccinimidyl 5- (and -6)-carboxytetramethylrhodamine (NHS-Rho) were purchased from Molecular Probes (Eugene, Oreg.). RPMI 1640, horse serum, 7H9 broth, 7H10 agar, and OADC (oleic acid, albumin, dextrose, and catalase) enrichment were from Fisher Scientific (Pittsburgh, Pa.). LB broth was from American Biorganics (Niagara Falls, N.Y.). Sephadex G-75, Enzyme-Free Cell Dissociation Solution, and zymosan A were from Sigma Chemical Co. (St. Louis, Mo.). Goat anti-horse immunoglobulin G (IgG)-biotin conjugates, avidin-fluorescein conjugates, and goat anti-mouse IgG-fluorescein conjugates were from Pierce (Rockford, Ill.). The monoclonal antidinitrophenol (DNP) antibody designated 29B5 was a gift of F. Brodsky, University of California at San Francisco, and was originally obtained (5) from L. Herzenberg (Stanford University). *M. avium* ATCC 49601 was obtained from the American Type Culture Collection (ATCC). *Salmonella typhimurium* 14028 was obtained from N. Buchmeier (Salk Institute, La Jolla, Calif.).

Measurement of optimum pH for *M. avium* survival. Flat, translucent colonies of *M. avium* were picked from 7H10 agar plates, and a suspension was grown in 7H9 broth supplemented with OADC. When a sufficient bacterial density was achieved, the suspension was centrifuged at 5,000 × *g* for 15 min, and the pellet was washed twice by centrifugation with sterile phosphate-buffered saline (PBS) containing 0.05% Tween 80 (PBS-T). Bacteria were dispersed in 7H9 broth adjusted to various pHs. One day after incubation, serial dilutions of bacteria in PBS were dispersed on 7H10 agar plates enriched with OADC and incubated at 37°C in 5% CO_2 and moist air. After 2 weeks, the number of CFU was determined by counting the number of bacterial colonies.

Labeling of bacteria or zymosan A with fluorescent probes. *M. avium* was cultured in 7H9 broth supplemented with OADC, and *S. typhimurium* was cultured in LB broth. Log-phase cultures were centrifuged at 5,000 × *g* for 15 min, washed twice in PBS, and resuspended in PBS containing 0.05% Tween-80. Zymosan A was opsonized by incubation in horse serum for 2 h, washed twice by centrifugation, and resuspended in PBS.

To label bacteria or zymosan A with fluorescent probes, NHS-CF and NHS-Rho solutions (100 μl of each at 0.2 mg/ml) were combined and added to 1 ml of a suspension containing 4×10^8 to 8×10^8 bacteria, and the suspension was vortexed for several seconds. The mixtures were incubated on ice for 30 min in the dark. Fluorescent bacteria or zymosan A was separated from free fluorescent dyes by gel filtration on Sephadex G-75.

Microscopy. The fraction of labeled bacteria was determined by video fluorescence microscopy with a silicon-intensified target camera (Cohu, Torrence, Calif.) and image processor (Perceptics, Knoxville, Tenn.) attached to a microscope (Zeiss). The total bacterial count was determined by observing multiple fields in white light by differential interference contrast microscopy, and fluorescent bacteria were counted under the appropriate illumination. The uniformity of labeling (i.e., the variability of Rho and CF intensities) and the uniformity of the CF/Rho ratio on individual bacteria were also determined. Filters used to detect CF fluorescence consisted of an excitation bandpass filter (450 to 490 nm), dichroic mirror (510 nm), and a longpass emission filter (>520 nm). Filters used to detect Rho fluorescence consisted of an excitation bandpass filter (536 to 556 nm), dichroic mirror (580 nm), and a longpass emission filter (>580 nm).

Viability and intracellular survival of fluorescent bacteria. The viability of fluorescent bacteria was determined by comparing the fraction of fluorescent bacteria, observed by microscopy, with the number of CFU in an equivalent volume. After the fraction of fluorescent bacteria was determined (as described above), bacteria were counted with a hemacytometer. Serial dilutions of the enumerated bacterial suspension were dispersed on 7H10 agar plates, and colonies were counted after 2 weeks.

In order to evaluate the effect of fluorescent labeling on cellular uptake and intracellular survival within macrophages, J774 cells were cultured in RPMI 1640 medium supplemented with 5% fetal and 5% newborn bovine sera (referred to as complete medium). Replicate cultures of J774 cells were overlaid with a bacterial suspension adjusted to yield a bacterium/cell ratio of 100:1. The cells were infected for 1 h and washed three times with PBS to eliminate unbound bacteria. Infected J774 cells were refed with complete RPMI 1640 medium. At various time points, the cells were washed again with PBS and lysed with 1 ml of 0.25% sodium lauryl sulfate in PBS. The cell lysates were diluted serially, and 100 μl of each dilution was plated in duplicate on 7H10 agar plates.

Measurement of environmental pH of bacteria in J774 cells. (i) Fluorometry. J774 cells grown in monolayer culture were harvested with Enzyme-Free Cell Dissociation Solution (Sigma) and plated at a density of 10^6 cells per 96-mm^2 culture dish. After overnight incubation in complete medium, cells were infected for 1 h by adding bacteria to cells at a ratio of 100 bacteria per cell. After infection, cells were washed three times with complete RPMI medium to eliminate extracellular bacteria and returned to complete medium. At various time points, the cells were washed with PBS and suspended in 2 ml of PBS. The CF and Rho fluorescence emission intensity was measured immediately with an SLM 8000-C spectrofluorometer (SLM, Chicago, Ill.). The CF/Rho fluorescence ratio varies with pH, and ratios were mapped to pH by using the following in situ calibration method.

For in situ calibration for calculation of pH from the CF/Rho emission ratio, J774 cells infected with fluorescent *M. avium* were suspended in buffers having a defined pH over the range of pH 4.0 to pH 7.4. Buffers contained 50 mM methylamine to collapse pH gradients across membranes (12, 15) and clamp the intracellular pH to the extracellular pH. The fluorescence intensity was measured at an excitation wavelength (λ_{ex}) of 490 nm and emission wavelength (λ_{em}) of 520 nm for CF and an λ_{ex} of 540 nm and λ_{em} of 580 nm for Rho. The calibration curve was obtained by plotting the CF/Rho fluorescence intensity ratio versus pH.

(ii) Video fluorescence microscopy. J774 cells cultured on glass coverslips were infected (as above) with CF/Rho-labeled *M. avium*. At intervals, each coverslip was rinsed sequentially with culture medium and PBS to remove extracellular bacteria and placed in a coverslip holder that allowed immersion of the cells in PBS during observation. For each sample, a pair of images was acquired: one at wavelengths appropriate for CF, and the other at wavelengths appropriate for Rho. A dual-wavelength dichroic mirror (510 to 530 nm and 560 to 650 nm bandpass) was used to reduce the image misregistration that would be introduced by changing dichroic filters. The images were acquired with an intensified charge-coupled device camera and image digitizer (Quantex, Woburn, Mass.). Out-of-focus background images were taken at the CF and Rho wavelengths and subtracted from the corresponding images. Each CF image was divided by the paired Rho image, and the resulting fraction was scaled to a range of 0 to 255 to allow display as an 8-bit image.

For in situ calibration for calculation of pH from the CF/Rho emission ratio, infected J774 cells on coverslips were incubated for 6 to 10 min in methylamine-containing PBS that was adjusted to various pHs in the range from pH 4.0 to 7.5. The methylamine concentration was 50 mM. Pairs of CF and Rho images were acquired and processed as above, yielding ratio images. All fluorescent objects of intensity greater than background were identified by the software, and the ratio for each was recorded. Multiple images were analyzed at each pH (total n, ≥50 objects). The ratios for each object at each pH were averaged to give a mean fluorescence ratio for each pH, and the standard deviation was calculated as an indication of the variability around each value. The mean ratio was plotted as a function of pH, thus providing a ratio/pH calibration curve. Because of variability in labeling efficiency and data acquisition parameters, calibration curves were determined for each experiment.

(iii) Confocal laser scanning microscopy. *M. avium*-infected J774 cells were prepared as described above for video fluorescence microscopy. An argon ion laser was used to excite CF at 488 nm and Rho at 514 nm. Pairs of CF and Rho images were obtained as described for video fluorescence microscopy except that cells were optically sectioned along the Z (vertical) axis by acquiring 10 to 15 image pairs at depth intervals of 0.5 μm. The instrument used was an Olympus microscope and laser confocal scanning unit, driven by custom software on a Windows-based microcomputer. The software was written and maintained by the Advanced Microscopy Imaging Laboratory at SUNY Buffalo.

Images were transported to a Macintosh computer and processed with NIH_image software (authored by W. Rasband, National Institutes of Health; obtained by anonymous FTP [file transfer protocol] from zippy.nimh.nih.gov). A custom macroroutine was written to automate the processing of multiple pairs of images as described below.

Each confocal image was smoothed by using a 3 × 3 deconvolution mask in order to reduce the relatively high pixel-to-pixel intensity variation that would be amplified by the ratio calculation. After smoothing, the background intensity was determined from blank (i.e., extracellular) regions in the CF and the Rho images, and this background was subtracted from all images in the data set. Because spurious ratios are obtained from object edges or regions where there is slight misalignment of fluorescence in the CF and Rho channels (produced by Brownian motion, motility of intracellular organelles, or optical effects), a binary mask was prepared from each CF and Rho image by choosing a threshold that excluded all fluorescence dimmer than the bacteria. The CF and Rho masks were then combined by using a Boolean AND operation to produce a composite mask,

thereby removing all but the fluorescent signal common to both images. The composite mask was applied individually to the CF and Rho images of each pair, and the resulting images were then divided to produce a ratio, rescaled, and mapped to pH values as described above for video fluorescence microscopy.

Preparation of opsonized and antibody-coated *M. avium*. (i) Opsonization of *M. avium*. Five milliliters of an *M. avium* suspension (optical density of 0.7 to 0.8 at 600 nm) was centrifuged at 5,000 × *g* for 15 min and washed twice with PBS-Tween. The bacterial pellet was dispersed in 5 ml of horse serum, incubated for 1 h at 36°C, and rinsed twice with PBS-T. The binding of horse IgG to the surface of *M. avium* was confirmed by fluorescence microscopy with biotinylated goat anti-horse IgG and avidin-fluorescein.

(ii) Coating of *M. avium* with anti-DNP IgG. Bacteria were washed as described above and dispersed in 1 ml of PBS-T, and 0.2 mg of the NHS ester of DNP was added. The suspension was incubated for 30 min on ice to derivatize *M. avium*. DNP-labeled *M. avium* was separated from unreacted DNP by gel filtration on Sephadex G-75, with a mobile phase of PBS-T. A 1-ml aliquot of DNP-labeled *M. avium* was incubated for 1 h with a 1:50 dilution of 29B5, a monoclonal mouse anti-DNP antibody. The binding of mouse anti-DNP to DNP-labeled *M. avium* was confirmed by fluorescence microscopy with a polyclonal fluorescein-goat anti-mouse IgG antibody.

Measurement of phagosome-lysosome contents colocalization by confocal laser scanning microscopy. Secondary lysosomes of J774 cells were labeled via fluid-phase pinocytosis by incubating J774 cells overnight in the presence of 25 μM calcein. The cells were then washed with PBS and infected for 1 h with Rho-labeled *M. avium* that was either live or heat killed by incubation at 70°C for 2 h. Infected J774 cells were examined by confocal laser scanning microscopy at an excitation wavelength of 488 nm to observe calcein-labeled lysosomes or at 514 nm to observe phagosomes containing Rho-labeled *M. avium*. Fluorescence images were processed with NIH_image software and a macro programmed to count automatically the number of distinct and colocalized regions of Rho and calcein fluorescence.

Statistics. Data are expressed as the mean ± standard error (SE). The significance of differences in pH measured for live and heat-killed *M. avium* was assessed with the unpaired, two-tailed Student's *t* test. Results were termed significant at $P < 0.05$. The significance of differences in phagosome pH measured for *M. avium*, *S. typhimurium*, and zymosan was tested by one-way analysis of variance (ANOVA). The significance of differences in phagosome pH measured for *M. avium* and antibody-coated *M. avium* also was tested by ANOVA.

RESULTS

Labeling of *M. avium* with fluorescent probes. We investigated two approaches to develop a covalent labeling method that gives a high efficiency of labeling without a reduction in the viability of bacteria: (i) generation of aldehydes on the surface of bacteria via periodate oxidation, followed by conjugation with hydrazide-activated fluorescent dyes, and (ii) conjugation of intrinsic bacterial surface amines with NHS esters of fluorescent dyes. Of these two methods, the first was associated with significant loss in bacterial viability, and the second proved to be more suitable. By fluorescence microscopy, typically 83% ± 9% of the NHS-derivatized bacteria showed CF fluorescence, and 74% ± 13% showed Rho fluorescence (data not shown). Fluorescence appeared to be distributed uniformly on bacteria.

The viability of dye-labeled *M. avium* was compared with that of nonlabeled bacteria. In one representative experiment, 87% ± 3% of the nonlabeled bacteria and 81% ± 8% of the labeled bacteria formed colonies on 7H10 agar (data not shown).

Cellular uptake and survival within macrophage-like J774 cells were compared for labeled and nonlabeled bacteria. After a 3-h incubation and extensive washing, J774 cells infected at the same ratio of bacteria per cell showed 28 ± 8 and 19 ± 2 CFU per cell for fluorescent and nonfluorescent *M. avium*, respectively (data not shown). The difference in the cellular uptake of *M. avium* was not statistically significant. Intracellular survival of bacteria, evaluated 2 and 5 days after infection, showed no significant difference between labeled and nonlabeled *M. avium* (data not shown).

Environmental pH of cell-associated bacteria determined by spectrofluorometry. To determine the population-averaged pH to which cell-associated *M. avium* bacteria were exposed in J774 cells, the CF/Rho fluorescence ratio from labeled *M. avium* was measured at various intervals after infection. The CF/Rho ratio declined rapidly, and a pH of 5.8 was achieved 15 min after infection (Fig. 1). The pH value calculated from *M. avium*-associated probes remained at pH 5.6 to 5.8 over the succeeding 6 h, suggesting no further acidification of the *M. avium*-containing compartment.

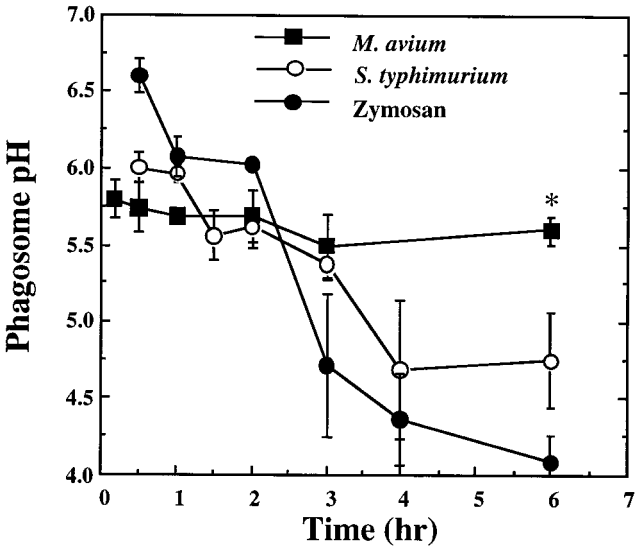

FIG. 1. Phagosomal pH as determined from fluorophore-labeled bacteria and zymosan. Replicate cultures of J774 cells were incubated for 1 h with live *M. avium*, *S. typhimurium*, or zymosan particles that were covalently labeled with CF and Rho, as indicated. At intervals, the average pH indicated by the fluorophores was determined by fluorescence spectroscopy. Each point represents the mean ± SE for three experiments. *, significant differences among groups at $P < 0.01$ by ANOVA.

For comparison, J774 cells were exposed to similarly labeled *S. typhimurium* or zymosan A (Fig. 1). Fluorophores linked to *S. typhimurium* indicated a pH of 6.0 at 30 min after infection and showed continuing acidification of the bacterial environment with time. At 6 h after infection, the pH was 4.75. *S. typhimurium* is known to survive within macrophages, and fluorescent bacteria were found to survive and proliferate within J774 cells as efficiently as did nonlabeled bacteria (data not shown). Zymosan A was used as a marker for a biodegradable particle routed to secondary lysosomes. Fluorophores associated with zymosan A indicated an environmental pH of 6.6 at 30 min after infection and showed that the environment continued to acidify. At 6 h, zymosan A was exposed to an average environmental pH of <4.5, according to the covalently attached fluorophores.

To test whether a heat-labile property was involved in the disposition of *M. avium* to a less-acidic intracellular compartment, the environmental pH encountered by live and heat-killed *M. avium* cells was compared (Fig. 2A). At 30 min after infection, fluorophores associated with either population indicated a pH of approximately 5.8. At 6 h after infection, heat-killed bacteria resided at pH 4.8, significantly more acidic than observed for live bacteria. Overall, heat-killed *M. avium* cells encountered an environment that acidified with kinetics and extent similar that in which intracellular *S. typhimurium* or zymosan A resided (cf. Fig. 1 with Fig. 2A).

Quantitation of pH in individual phagosomes by video fluorescence microscopy. The results obtained by fluorometry represent a population-averaged pH that includes signals from both cell-associated and extracellular bacteria. Rates of acidi-

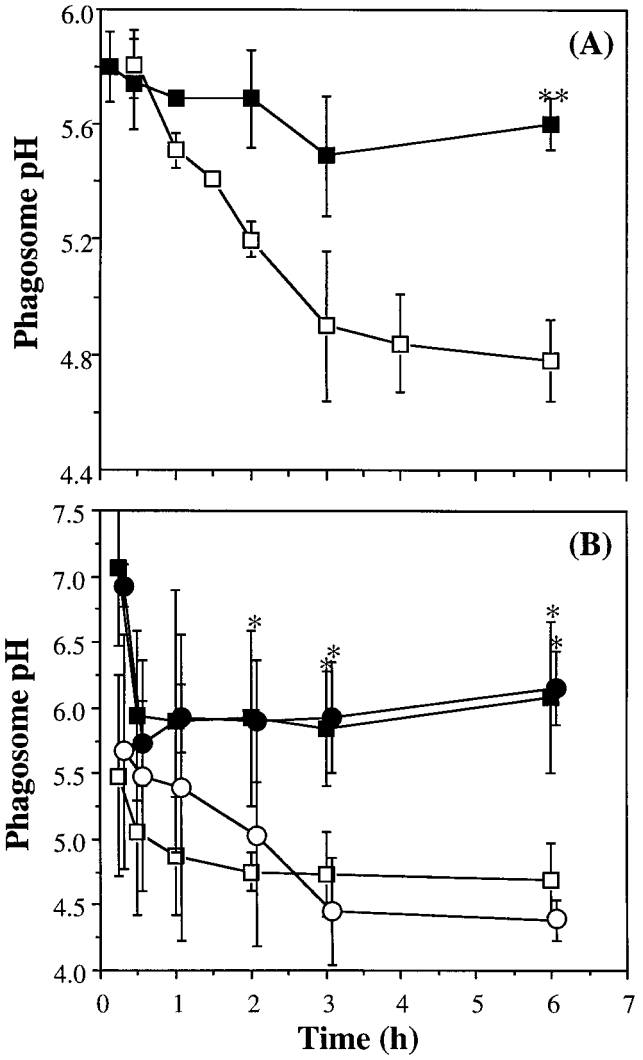

FIG. 2. Phagosomal pH encountered by live and heat-killed *M. avium*. J774 cells were infected with live or heat-killed *M. avium* cells that had been labeled covalently with CF and Rho. At intervals, the cell-associated fluorescence was measured, and pH was calculated from the CF/Rho ratio. (A) J774 cells were suspended in buffer, and fluorescence was measured by fluorometer. **, differences significant at $P < 0.01$ by Student's *t* test. ■, live *M. avium*; □, heat-killed *M. avium*. (B) J774 cells on coverslips were observed by video fluorescence microscopy (VFM) or confocal laser scanning microscopy (CLSM), and images were acquired at the appropriate wavelengths for CF and Rho. pH was calculated by dividing each CF image by the corresponding Rho image and then mapping the ratio to pH by using a standard curve. pH was recorded for each distinct fluorescent object (>50 counted), and each point represents the calculated mean. The SD represents the heterogeneity of pHs encountered by individual intracellular bacteria. *, differences significant at $P < 0.001$ by Student's *t* test. ■, live *M. avium*, VFM data acquisition; ●, live *M. avium*, CLSM data acquisition; □, heat-killed *M. avium*, VFM data acquisition; ○, heat-killed *M. avium*, CLSM data acquisition. CLSM data are offset by 5 min on the abscissa for clarity.

fication may be biased toward neutral pH if cell surface binding occurs without subsequent phagocytosis of the labeled bacteria. Therefore, we employed video fluorescence microscopy to examine the heterogeneity of environments to which *M. avium* cells were exposed in J774 cells. Images of cells were acquired at the appropriate wavelengths for CF and Rho and ratioed, and the pH was calculated for each individual fluorescence accretion within cells. At early times after infection, both heat-killed and live *M. avium* cells resided in compartments of heterogeneous pH, as indicated by the large SE calculated for all cell-associated bacteria (Fig. 2B). As infection progressed, the heterogeneity of pH decreased. Approximately 6 h after infection, the observed heterogeneity of pH was minimal for both live and heat-killed bacteria. Over the time course observed, the mean pH was similar to that observed by fluorometry (Fig. 2A); on the average, live *M. avium* encountered an environmental pH of 6.0 at 6 h after infection, slightly lower than the pH determined by fluorometry. Heat-killed *M. avium* was exposed to a mean pH of 4.7, also slightly more acidic than the pH determined by fluorometry.

The rate of acidification appeared to be more rapid when investigated by fluorescence microscopy than by fluorometry. Nadir pH values were observed by microscopy within 30 to 60 min of infection. By fluorometry, the pH nadir for heat-killed *M. avium* was achieved at 3 h. Given the heterogeneity of pH observed by microscopy and the lower rate of acidification observed by fluorometry, it appears that the fluorometry results may be biased by bacteria in less-acidic compartments.

Quantitation of pH in individual phagosomes by confocal laser scanning microscopy. The events surrounding phagocytosis of *M. avium* were investigated by confocal laser scanning microscopy, both to achieve better spatial resolution of intracellular bacteria and cellular organelles and to take advantage of the wider dynamic range of the instrument. Figure 3 shows the CF/Rho ratio calculated from images taken 6 h after infection. A gray scale was assigned to the observed CF/Rho ratios, and the scale was mapped to pH by using an in situ pH calibration method (described in Materials and Methods). Similar to the observations made at low light levels by video fluorescence microscopy, confocal laser scanning microscopy showed that live *M. avium* resided in a less acidic environment than did heat-killed *M. avium*. The pH of individual fluorescent accretions was recorded and analyzed; Fig. 2B summarizes the data for the cell-associated bacteria from numerous cells. The large standard deviation in pH at ≤1 h demonstrates the heterogeneous distribution of pH for cell-associated bacteria early in infection. As infection progressed, the heterogeneity of environmental pH diminished. Consistent with the data obtained by fluorometry and fluorescence microscopy, live *M. avium* resided in phagosomes of pH 6.1 at 6 h after phagocytosis, whereas heat-killed *M. avium* resided in phagosomes of pH 4.5.

Optimal pH for *M. avium* survival and growth. To investigate the ramifications of phagosomal pH with respect to the intracellular survival of *M. avium*, bacterial viability was examined after overnight incubation of replicate cultures in simple broths adjusted to various pHs. The survival of *M. avium* was pH sensitive, and the number of CFU was greatest at pH 6.0 (Fig. 4). Thus, the environmental pH encountered by intracellular *M. avium* was close to the optimal pH for survival and growth in simple broths.

Role of cell surface receptors in determining pH encountered by *M. avium*. The quantitative studies with fluorometry, video fluorescence microscopy, and confocal laser scanning microscopy consistently showed that the phagosomal pH to which live *M. avium* was exposed in macrophages was less acidic than the environment to which heat-killed *M. avium* was exposed. We hypothesized that the receptor by which *M. avium* enters cells may direct live bacteria into a less acidic compartment, as has been observed for other intracellular pathogens. The hypothesis was challenged by targeting *M. avium* to cell surface Fc or opsonin receptors in an attempt to route bacteria to a low-pH compartment. Bacteria were opsonized nonspecifically with horse serum or derivatized covalently with a synthetic antigen and then decorated specifically with monoclonal

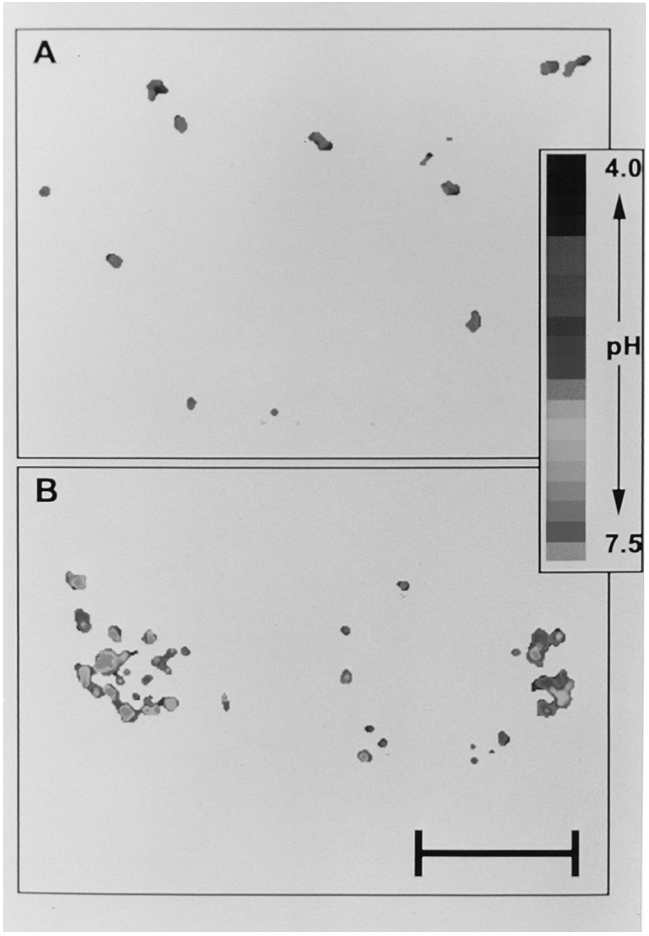

FIG. 3. Intracellular distribution of live and heat-killed *M. avium*. J774 cells were infected as described in the text with fluorescent heat-killed (A) or live (B) *M. avium*. Six hours after infection, CF and Rho images of the cells were acquired by confocal laser scanning microscopy at the appropriate wavelengths. Cells were sectioned optically in the Z plane, with a slice thickness of 0.5 μm. The images were processed as described in the text to indicate the pH encountered by cell-associated fluorescent bacteria. The gray scale displays pH (derived from the ratio of fluorophore intensities). Each gradation represents a difference of approximately 0.175 pH unit. Bar, ~5 μm.

antibodies. Following either treatment, bacteria were tested for binding of immunoglobulin by indirect immunofluorescence. In both cases, bacteria were labeled heavily (data not shown). The number of viable cell-associated bacteria was determined by measuring CFU after infecting, washing, and lysing J774 cells, as described in Materials and Methods. Opsonization with horse serum increased cellular uptake of bacteria threefold, while coating of DNP-bearing bacteria with anti-DNP increased bacterial uptake sevenfold (data not shown). Figure 5 shows that there was no significant difference in the intracellular environmental pH encountered by unopsonized, opsonized, or antibody-coated *M. avium* cells.

Phagosome-lysosome fusion in *M. avium*-infected cells. To test whether the less acidic environmental pH encountered by live *M. avium* involved a reduction in phagosome-lysosome fusion, we investigated the colocalization of phagosomes containing fluorescent *M. avium* with fluorescent lysosomes. Confocal laser scanning microscopy images show that nearly all Rho-labeled, heat-killed *M. avium* colocalized with calcein-labeled lysosomes (data not shown). In contrast, live Rho-labeled *M. avium* showed an intracellular localization distinct

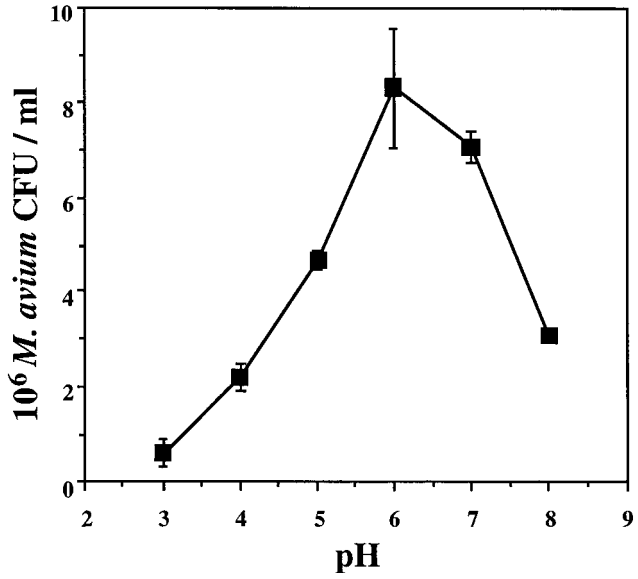

FIG. 4. pH-dependent survival of *M. avium* in vitro. Log-phase cultures of *M. avium* in 7H9 broth were adjusted to various pHs and incubated overnight at 35°C. Subsequently, serial dilutions of each bacterial culture were spread on 7H10 agar plates, and colonies of *M. avium* were counted after 2 weeks of incubation at 35°C. Each point represents the mean ± SE (three experiments, two replicates per experiment).

from labeled lysosomes (data not shown). Quantification of multiple image pairs showed that 98% of all heat-killed *M. avium* colocalized with calcein-labeled lysosomes, whereas 18% showed colocalization in the absence of heat treatment (data not shown). Interestingly, 80 to 90% of labeled bacteria

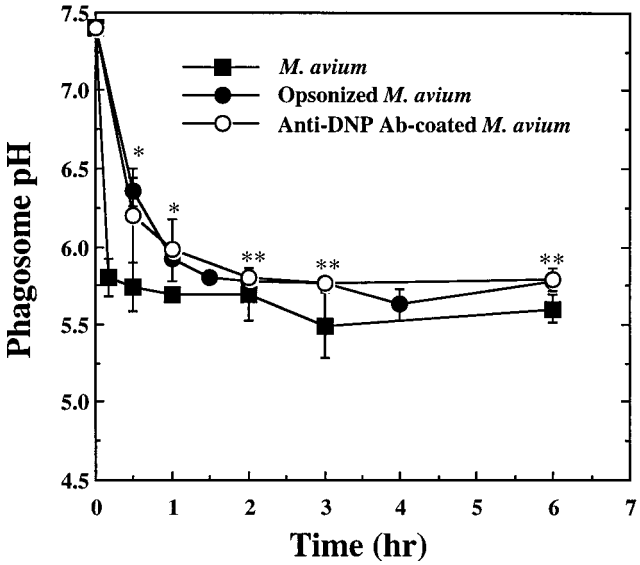

FIG. 5. Intracellular pH encountered by opsonized and antibody-coated *M. avium*. Replicate cultures of J774 cells were infected in complete medium with dual-labeled fluorescent *M. avium* opsonized with horse serum, unopsonized, or coated with anti-DNP IgG after covalent derivatization of the bacteria with DNP. The environmental pH of cell-associated bacteria was determined by spectrofluorometry from the ratio of the CF and Rho fluorescence intensities, using an in situ calibration curve (described in the text). Each point represents the mean pH ± SE (three experiments). Data for *M. avium* are redrawn from Fig. 1 to enable comparison. *, no significant differences among groups at $P > 0.05$ by ANOVA; **, no significant differences among groups at $P > 0.5$ by ANOVA.

were capable of colony formation in the absence of heat treatment, suggesting that some fraction of the 18% colocalized may be nonviable bacteria in the samples that were not heat treated.

DISCUSSION

The acidification of bacterium-containing phagosomes is a major contributor to the antimicrobial mechanisms of macrophages. To survive, intracellular pathogens must adapt to live in an acidic environment, inhibit the acidification process, or escape the phagolysosome to a neutral environment. To investigate the contributions of these mechanisms to the intracellular survival of *M. avium*, bacteria were labeled with dual fluorescent probes, pH-sensitive CF and pH-insensitive Rho. The use of NHS esters of these fluorescent dyes gave a high labeling yield and did not reduce bacterial viability or intracellular survival capacity. Because a large fraction of bacteria were labeled (typically 75 to 83%), the signal contributed by nonlabeled, viable bacteria was minimized.

By fluorometry, we observed that the phagosomal pH enveloping *M. avium* differed markedly from that encountered by intracellular *S. typhimurium*, zymosan A, or heat-killed *M. avium*. At 6 h after infection, viable *M. avium* resided at a pH of approximately 5.7, while *S. typhimurium*, zymosan A, and heat-killed *M. avium* resided at pH <4.8. The continuing, gradual acidification observed for *S. typhimurium*-containing vesicles agrees well with a previous report (1), and the contrasting fates of *S. typhimurium* and *M. avium* suggest the diversity in survival strategies that intracellular pathogens may employ.

The microscopic spectroscopy approaches used are unique in their ability to demonstrate the heterogeneity of pH among phagosomes. Video fluorescence microscopy and confocal laser scanning microscopy showed that, on the average, individual phagosomes containing live *M. avium* were less acidic than those containing heat-killed *M. avium*. The heterogeneity observed shortly after infection may result from asynchrony in the various phases of bacterial invasion, such as binding to cells, internalization, and phagosome-lysosome fusion. The more homogeneous distribution of pH observed after 6 h suggests that most bacteria eventually reside in similar environments.

Our observation that live but not heat-killed *M. avium* cells reside in a less acidic environment both corroborates and extends previous work. It was observed by electron microscopy that dead *M. avium* cells colocalized with markers for acidic lysosomal compartments (6). Recently, Sturgill-Koszycki et al. (17) reported that live *M. avium* in murine bone marrow macrophages colocalize with phagosomes of pH 6.3 to 6.5, whereas zymosan and *Leishmania* organisms resided in phagosomes of pH <5.0. A precedent for the effect of viability on intracellular fate is previous work (9) in which opsonized live *Legionella pneumophila* cells were observed to reside in phagosomes of pH 6.1, whereas dead *L. pneumophila* cells resided at pH 5.2.

The less acidic phagosomal pH encountered by *M. avium* approximates closely the optimal pH for survival and growth of *M. avium* in simple broths and is similar to the optimal pH reported for *Mycobacterium tuberculosis* and *Mycobacterium scrofulaceum*, pH 6 to 6.5 (4). The residence of *M. avium* at an ambient phagosomal pH of 5.8 to 6.1 and the optimal survival of *M. avium* in pH 6.0 suggest collectively that the less acidic environment encountered by *M. avium* within macrophages favors its survival.

Several receptor systems are implicated in the entry of *M. avium* into macrophages and macrophage-like cells, including fibronectin, complement, and mannosyl-fucosyl receptors (3). The important role of receptors in determining the intracellular fate of bacteria has been demonstrated for several organisms, including *Toxoplasma gondii* and *M. tuberculosis. M. tuberculosis* was observed in lysosomal vesicles after entry via Fc receptors but not via CR3 receptors (2). It was also observed that *T. gondii* opsonized with specific antibody entered an acidified phagolysosome, whereas nonopsonized *T. gondii* entered a less-acidified, nonfused compartment (10). Given the interesting mechanistic and therapeutic ramifications of perturbations that may alter the intracellular fate of *M. avium*, we opsonized bacteria with serum or decorated bacteria specifically with immunoglobulin. We found little difference in the environmental pH encountered by opsonized and nonopsonized *M. avium*. Thus, uptake into cells via the Fc receptors or nonspecific opsonin receptors may not play an important role in determining the intracellular environment to which *M. avium* is exposed. Alternatively, the strategies employed here for altering the pathway of uptake were unable to override the inherent receptor targeting mechanisms unique to live *M. avium*.

The fusion of phagosomes with lysosomes delivers proton-pumping activity to the phagosome, and a less acidic phagosomal pH may be one consequence of an inhibition of membrane fusion (1, 10). The results presented here support the hypothesis that the presence of live *M. avium* significantly reduces phagosome-lysosome interaction. In contrast, the nearly complete colocalization of heat-killed fluorescent *M. avium* with fluorescently labeled secondary lysosomes suggests abundant fusion of *M. avium*-containing vacuoles with lysosomes. Our results are consistent with recent work (17) showing that phagosomes containing *M. avium* had a reduced content of a proton-ATPase that is contributed via fusion. Although the controls of phagosome-lysosome fusion are poorly understood, some previous reports suggest that the less acidic pH of phagosomes per se would not inhibit fusion directly (11). Our data suggest either a heat-labile bacterial component or some more complex mechanism dependent upon viable bacteria as the mechanistic basis for reduced phagosome-lysosome colocalization.

ACKNOWLEDGMENTS

We thank H. A. Berman (SUNY Buffalo) for the use of the fluorometer, J. A. Swanson (Harvard) for his advice in preparation of the manuscript, and F. Brodsky (UC San Francisco) for the anti-DNP antibody. P. C. Cheng (Advanced Microscopy Imaging Laboratory, SUNY Buffalo) is thanked for advice with and access to the confocal laser scanning microscope, and N. Buchmeier is thanked for kindly supplying several *Salmonella* strains.

This work was supported by grant AI28237 from the National Institutes of Health.

REFERENCES

1. **Alpuche-Aranda, C. M., J. A. Swanson, W. P. Loomis, and S. I. Miller.** 1992. *Salmonella typhimurium* activates virulence gene transcription within acidified macrophage phagosomes. Proc. Natl. Acad. Sci. USA **89:**10079–10083.
2. **Armstrong, J. A., and P. D. Hart.** 1975. Phagosome-lysosome interactions in cultured macrophages infected with virulent tubercle bacilli: reversal of the usual nonfusion pattern and observations on bacterial survival. J. Exp. Med. **142:**1–16.
3. **Bermudez, L. E., L. S. Young, and H. Enkel.** 1991. Interaction of *Mycobacterium avium* complex with human macrophages: roles of membrane receptors and serum proteins. Infect. Immun. **59:**1697–1702.
4. **Chapman, J. S., and J. S. Bernard.** 1962. The tolerances of unclassified mycobacteria. I. Limits of pH tolerance. Am. Rev. Respir. Dis. **86:**582–583.
5. **Chin, D. J., R. M. Straubinger, S. Acton, I. Näthke, and F. M. Brodsky.** 1989. 100 kDa polypeptides in peripheral clathrin-coated vesicles are required for receptor-mediated endocytosis. Proc. Natl. Acad. Sci. USA **86:**9289–9293.
6. **Crowle, A. J., R. Dahl, E. Ross, and M. H. May.** 1991. Evidence that vesicles containing living virulent *Mycobacterium tuberculosis* or *Mycobacterium avium* in cultured human macrophages are not acidic. Infect. Immun. **59:** 1823–1831.

7. **Ellner, J. J., M. J. Goldberger, and D. M. Parenti.** 1991. *Mycobacterium avium* infection and AIDS: a therapeutic dilemma in rapid evolution. J. Infect. Dis. **163:**1326–1335.
8. **Falkow, S., R. R. Isberg, and D. A. Portnoy.** 1992. The interaction of bacteria with mammalian cells. Annu. Rev. Cell Biol. **8:**333–363.
9. **Horwitz, M. A., and F. R. Maxfield.** 1984. *Legionella pneumophila* inhibits acidification of its phagosome in human monocytes. J. Cell Biol. **99:**1936–1943.
10. **Joiner, K. A., S. A. Fuhrman, H. M. Miettinen, L. H. Jasper, and I. Mellman.** 1990. *Toxoplasma gondii*: fusion competence of parasitophorus vacuole in Fc receptor transfected fibroblasts. Science **249:**641–646.
11. **Kielian, M. C., and Z. A. Cohn.** 1982. Intralysosomal accumulation of polyanions. II. Polyanion internalization and its influence on lysosomal pH and membrane fluidity. J. Cell. Biol. **93:**875–882.
12. **Maxfield, F. R.** 1982. Weak bases and ionophores rapidly and reversibly raise the pH of endocytic vesicles in cultured mouse fibroblasts. J. Cell Biol. **95:**676–681.
13. **Maxfield, F. R.** 1989. Measurement of vacuolar pH and cytoplasmic calcium in living cells using fluorescence microscopy. Methods Enzymol. **173:**745–771.
14. **Murphy, R. F., S. Powers, and C. R. Cantor.** 1984. Endosome pH measured in single cells by dual fluorescence flow cytometry: rapid acidification of insulin to pH 6. J. Cell Biol. **98:**1757–1762.
15. **Ohkuma, S., and B. Poole.** 1978. Fluorescent probe measurement of the intralysosomal pH in living cells and the perturbation of pH by various agents. Proc. Natl. Acad. Sci. USA **75:**3327–3331.
16. **Sibley, L. D., E. Weidner, and J. L. Weidner.** 1985. Phagosome acidification blocked by intracellular *Toxoplasma gondii*. Nature (London) **325:**416–419.
17. **Sturgill-Koszycki, S., P. H. Schlesinger, P. Chakraborty, P. L. Haddix, H. L. Collins, A. K. Fok, R. D. Allen, S. L. Gluck, J. Heuser, and D. G. Russell.** 1994. Lack of acidification in *Mycobacterium* phagosomes produced by exclusion of the vesicular proton-ATPase. Science **263:**678–681.
18. **Young, L. S.** 1988. *Mycobacterium avium* complex infection. J. Infect. Dis. **157:**863–867.

Editor: R. E. McCallum